Numerical study of cavitating structure near wake of a circular cylinder

[1,2] Pankaj Kumar*; [1]Dhiman Chatterjee; [1]Shamit Bakshi

[1]*Department of Mechanical Engineering, IIT Madras, Chennai 600 036*

[2]*Department of Mechanical Engineering, SRM University, Kattankulathur, Chennai 603203*

Abstract

A study of the existing literature on flow past circular cylinder reveals that less work has been reported in the upper sub-critical flow regime which corresponds to Reynolds number (Re_D) in the range $2x10^4 < Re_D < 2x10^5$. Hence, this work brings out the flow features in the near wake of a cylinder for a sub-critical flow regime under non-cavitating as well as under different cavitating conditions. A three-dimensional numerical study of flow around a circular cylinder was carried out at $Re_D=6.4x10^4$ for a wide range of cavitation number ($1.06 \geq \sigma/\sigma_i \geq 0.5$). Unsteady Reynolds averaged Navier-Stokes (URANS) approach coupled with Schnerr-Sauer cavitation model available in ANSYS-Fluent was used for this purpose. With the help of fine mesh around the cylinder and choice of suitable time step size, this study identifies factors influencing the occurrence of cavitation and portrays dynamics of cavities downstream of the cylinder. As a part of the validation of the numerical approach, variations of mean pressure coefficient around the cylinder as well as mean and fluctuating coefficients of base pressure have been compared with experimental data available in literature and a good agreement between the two have been observed. With a reduction in cavitation number, cavitation activity extends downstream. Based on the fast Fourier transformation (FFT) of pressure and vapor fraction data, it can be concluded that vortex shedding is suppressed due to the formation of extended cavities in the wake. Another interesting observation is the interplay between flow turbulence and cavitation structures. Simulations indicate that with increasing downstream distance from $x/d=0.3$ (near the cylinder) to $x/d=3$ (away from the cylinder), pressure recovers and turbulent kinetic energy decreases in case of non-cavitating flow. However, in case of cavitating flow, turbulent kinetic energy is higher at the region of collapse of vapor pockets than that at near the cylinder which is lower than that corresponding to the non-cavitating case at the same location.

Keywords: Circular cylinder, sub-critical flow regime, turbulent kinetic energy.

Introduction

Flow around a circular cylinder has been studied extensively in the past as it exhibits rich flow physics like wake structures, shear layer interaction and boundary layer. Roshko [1] categorized flow based on Reynolds number (Re) as subcritical ($300 < Re < 3 \times 10^5$), critical ($3 \times 10^5 < Re < 3.5 \times 10^5$) and supercritical ($Re > 3.5 \times 10^5$). This categorization is now widely used in the literature [2-3]. The difference in flow separation occurring on the cylinder surface is the main reason for the distinctive features observed in each of these flow regimes. Different aspects and properties of this flow, like lift and drag forces, phenomenon of vortex shedding and effect of aspect ratio of cylinder was reported past [4-6] but most of the work falls in critical and super critical flow regime.

In comparison with non-cavitating flow past a circular cylinder, there has been relatively less research on cavitating flow past a circular cylinder. Furthermore, investigations have mostly examined the critical and supercritical flow regimes. It has been discussed, in the context of non-cavitating flow that for flow past a bluff body, instantaneous lowest pressure is not necessarily located on the surface but may also occur in the centre of a fully formed eddy in the wake. Thus, cavitation is most likely to originate in these places. Specifically, in case of circular cylinder, cavitation may initiate on the surface of the cylinder, in the shear layer or in the wake depending on the Reynolds number. Wykes [7] had observed the formation of cavity for a circular cylinder, for different flow regimes. He found that, for subcritical flow regime, the cavity inception took place in shear layer or wake whereas for critical flow regime, cavitation inception took place on the cylinder surface. For supercritical flow regime, the cavity formed a wedge-like structure. Ramamurthy and Bhaskaran [8] studied cavitating flow past a circular cylinder for varying blockage factors. They found that the wall interference effect was less at high cavitation number but at low cavitation number this effect was high and drag coefficient dropped rapidly with a reduction in cavitation number.

*Corresponding Author, Pankaj Kumar: pankaj20221@gmail.com

Ihara and Murai [9] conducted an experiment to measure mean and fluctuating pressure distributions around a circular cylinder for Re between 3.2 x 10^5 and 3.6 x 10^5 in critical flow regime. Matsudaira et al.[10] measured the cavity collapse pressure and intensity distribution in wake with help of pressure transducers for the range of 4.5 x 10^5 < Re < 6 x 10^5. They found that due to cavity collapse, high imperative forces appeared in a regular fashion in wake and it was closely related with Karman vortex shedding frequency. In the subcritical range of flow, cavitation damage test was done by Sato and Saito [11] on Shalnev-type venturi in which straight cylindrical pin is mounted at the throat of venturi. They found that with a decrease in cavitation number, cavity length increases and was accompanied by an increase in surface damage.

Cavitation being a two-phase phenomenon with varying phase change, it is very difficult to model and several attempts have been made in the past to address this issue. The bottom line is that cavitating flows are usually high Reynolds number flows. Accurate representation of turbulent cavitating flow is quite challenging and yet progressive. The homogeneous flow model [12-14] assumes the mixture of constituent phases to be a single fluid and the mixture flow is governed by only one set of equations. Here both the phases are assumed to be in thermal and mechanical equilibrium and the governing equations are conservation laws written for the mixture. The modeling process is simplified with the help of some basic assumptions like, both the phases are strongly coupled and moves with same velocity. As far as the numerical simulation of cavitating flow past a circular cylinder is concerned, there are only a few studies available in literature. Seo et al. [15] used density-based homogeneous equilibrium model solver in DNS to compute sound produced by cavitating flow over a 2D cylinder at a Reynolds number of *200*. They used mixture density as a function of void fraction, mass fraction, pressure and temperature of liquid and vapour phase. This model captures the formation, detachment, convection, and collapse of the cavitation bubble very well, besides the generation and propagation of the linear and non-linear waves in the entire field. They concluded that the main source of noise found in spectrum was the collapse of vapour cavities. Gnanaskandan and Mahesh [16] conducted LES simulation on cylindrical geometry at Re=*200 & 3900* for different cavitation stages. They used homogeneous mixture model and characteristic based filtering to solve compressible Navier Stokes equation. They found that cavitation phenomenon suppressed turbulence and three-dimensionality.

So above mentioned literature survey reveals that there is a lack of study for upper subcritical range ($2x10^4 < Re < 2x10^5$), especially in the near wake ($x/d = 10$). This lack is more pronounced in case of cavitating flow. The present work aims to address this gap with emphasis of turbulent energy interaction with cavities.

2. Computational Procedure

The described case was simulated by using CFD software ANSYS Fluent 14. The formation of cavity behind cylinder is governed by the combination of turbulence and cavitation. Thus, in this study, a combination of *k-ω-SST* turbulent model and Schnerr–Saur cavitation model was used to simulate the transient behavior of wake cavitation.

2.1. Governing Equations

The governing equations for unsteady, incompressible flow with constant fluid properties are:

$$\frac{\partial u_i}{\partial x_i} = 0 \tag{1}$$

$$\frac{\partial u_i}{\partial t} + u_j \frac{\partial u_i}{\partial x_j} = -\frac{\partial p}{\rho \partial x_i} + \frac{\partial}{\partial x_j}[\vartheta \frac{\partial u_i}{\partial x_j}] \tag{2}$$

For turbulent flow, the 'closure' is achieved with the help of a suitable turbulent model. Works of several researchers (e.g. Unal et al.[17]) show that *k-ω-SST* model of Menter [18] performs better than other turbulent models for flow past a circular cylinder. Hence in this work, *k-ω-SST* model is adopted.

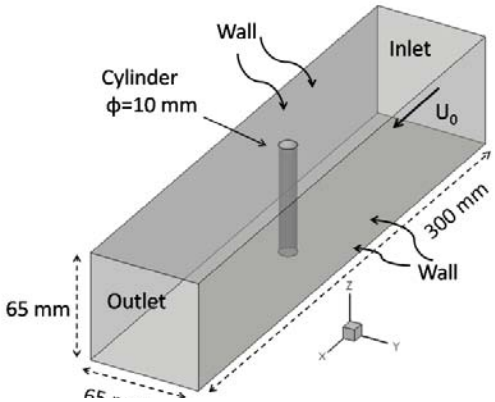

Figure 1: Computational domain showing the domain size, inlet, outlet and cylinder.

2.2. Computational Domains and Boundary Conditions

The choice of computational domain was mainly dictated by the experimental set up which is *65 mm x 65 mm* in cross-section and *300* mm long. A circular cylinder of length *65* mm was placed at the center of the computational domain shown in figure 1. A 3-D structured mesh was built in ICEM-CFD™ with multi-blocks using O-grids at the central block near the cylinder to ensure high density near the cylinder and wall. Proper attention was given to adjust the maximum and minimum acceptable angles (*126* and *54*), control skewness (*0.7 - 1*) and achieve an orthogonal quality of *0.9*. Total number of mesh elements of 4.43×10^5 is used in all the simulations obtained from grid independent. Unsteady simulation was carried out and time step sensitivity study was taken up to ascertain the effect of time step size. Based on the time-independent study, time step size of *100* μs was chosen and kept constant in all simulations. Uniform velocity was applied at the inlet and pressure condition was imposed at the exit of the domain. Side walls and cylinder surface were given a no-slip wall boundary condition. SIMPLE (Semi-Implicit Method for Pressure-Linked Equation) algorithm was used for pressure-velocity coupling. In spatial discretization, second order upwind scheme was used for momentum equation. Standard scheme was used for pressure terms and the quadratic upstream interpolation for convective kinetics (QUICK) scheme was used for vapor mass fraction transport equation. At each time step, the residue for all the equations solved was brought down to a convergence criterion of 10^{-5}. For each simulation, once the initial transience has decayed, *500* data files were stored for further post processing. MATLAB® was used to obtain mean and fluctuating contours of pressure, velocity, void fraction and turbulent kinetic energy.

3. Results and Discussion

Mean pressure coefficient ($\overline{C_P} = \frac{P_\theta - P_T}{\frac{1}{2}\rho v^2}$) was estimated for non-cavitating case. Comparison of numerical results with non-cavitating data is presented in figure 2(a). This serves as a validation of numerical simulation used for the present study. Mean pressure coefficient ($\overline{C_P}$) variation for different cavitation number is shown in figure 2(b) and shows that the surface pressure is influenced by cavitation. Here after angle *90°* ($\overline{C_P}$) is constant which confirms that separation angle is at *90°* for subcritical flow range [4]. The frequency obtained from pressure fluctuation ($C_P' = C_P - \bar{C}_P$) data at base point (at *180°* from front stagnation point) is *146* Hz. Strouhal number ($\frac{fD}{U}$) is obtained from this frequency is close to *0.2* which is also well validated for this range of Reynolds number [1, 19]. There is a very good agreement between the numerical prediction and experimental determination of the variation of Strouhal number with different cavitation numbers (figure 3(a)). The decrease in vortex shedding frequency is closely related with the elongation of cavity structure as reported by Young and Hall [20] and Ramamurthy and Bhaskaran [8]. Here the figure 3(b) brings out a comparison of instantaneous cavity and vortex structures and establishes the fact that wake cavitation is intricately related with vorticity dynamics.

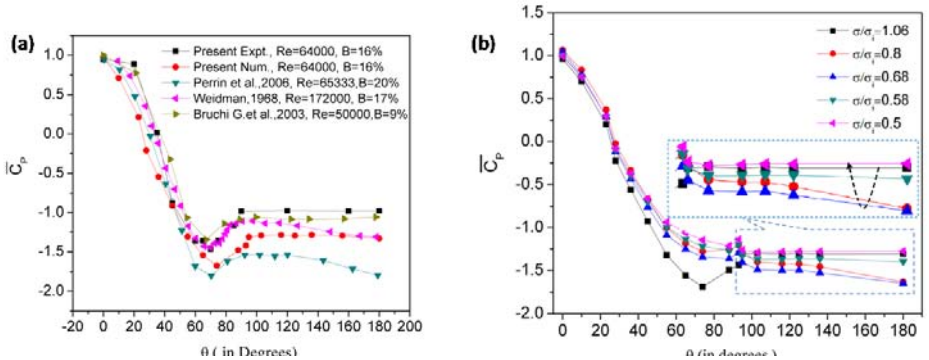

Figure 2: (a) Non-cavitating mean pressure coefficient (C_P) for $\sigma/\sigma_i=1.06$ (b) Mean pressure is plotted for different cavitation numbers. Present Expt. is referred to experiments conducted [19].

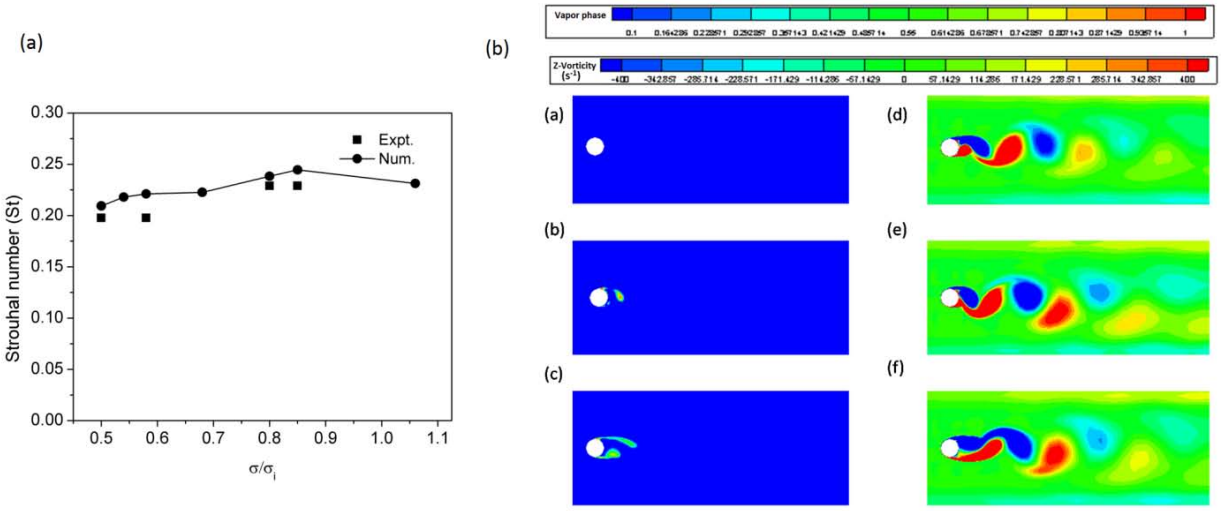

Figure 3: (a) Variation of Strouhal number obtained at base point (*180°*) for different cavitation numbers. "Expt." is pressure fluctuation at base obtained experimentally [21] whereas "Num." is pressure fluctuation at base obtained numerically. (b) Variation of vapour fraction and Z-vorticity obtained numerically for cavitation number (σ/σ_i) *1.06* (a & d), *0.58* (b & e) and *0.5* (c & f). Here (a),(b),(c) are instantaneous vapour fraction and (d),(e),(f) are corresponding vorticity contours.

The effect of cavity formation and collapse in the wake is studied in terms of turbulent kinetic energy of the cavitating flow. The mean vapour fraction together with mean turbulent kinetic energy contour is shown in figure 4 for different cavitation numbers (σ/σ_i) *0.85, 0.54* and *0.5*. Dashed line in this figure indicates the location of cavity collapse which is also the position where turbulent kinetic energy is high. The collapsing bubble produces pressure oscillations and increases turbulent kinetic energy locally. This phenomena is more clearly explained by time variation plots of pressure, turbulent kinetic energy and vapour fraction for non-cavitating flow (σ/σ_i = *1.06*) in figure 5. It is clear from figure 5(a) that moving from *x/d =0.6* to *x/d= 3,* pressure increases and turbulent kinetic energy decreases for non-cavitating flow. It also shows that near cylinder at *x/d=0.6*, temporal variations of pressure and turbulent kinetic energy are in phase but away from cylinder at *x/d =3*, they become out of phase. Figure 6 shows the time variation plots of pressure, turbulent kinetic energy and vapour fraction for cavitating flow (σ/σ_i *=0.5*). A closer look at figure 6(a) shows that a reduction in pressure is accompanied by an increase in volume fraction and conversely, a collapse in vapour volume accompanies a pressure rise. What is interesting is the fact that a rise in vapour volume also times well with low turbulent kinetic energy while a collapse of the cavity is followed by an increase in turbulent kinetic energy. In the non-cavitating case, (figure 5), an increase in downstream distance

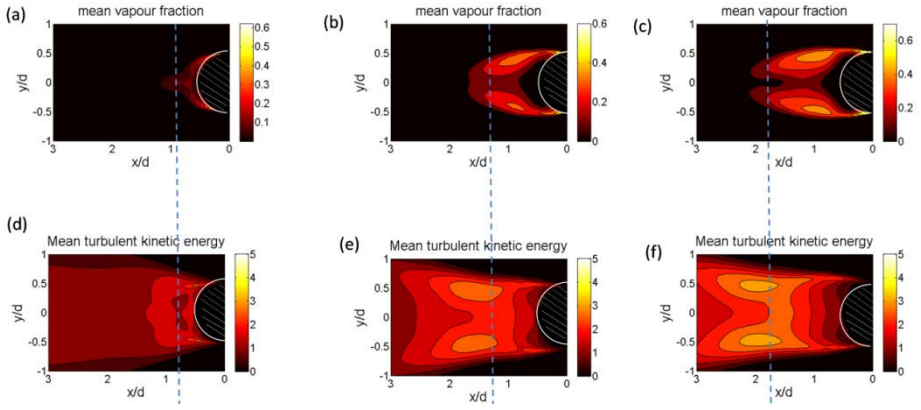

Figure 4: Mean contour of turbulent kinetic energy and vapour fraction shown for different cavitation number (σ/σ_i) : *(a, d) 0:85, (b, e) 0:54, (c, f) 0:5*. Dashed vertical lines shows the position of cavity collapse as well peak of turbulent kinetic energy.

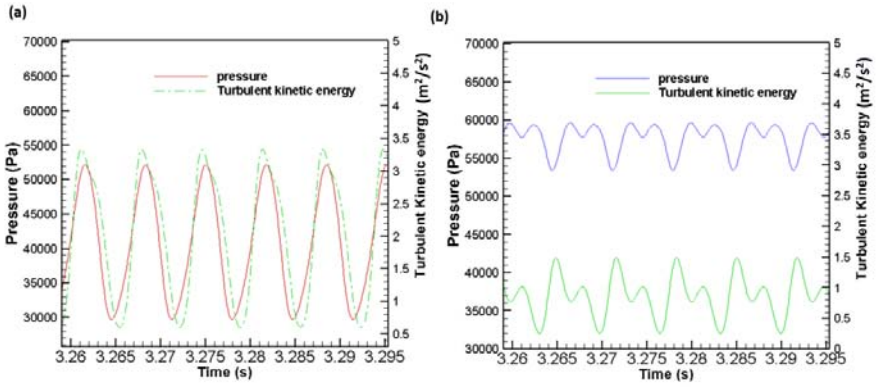

Figure 5: Variation of pressure and turbulent kinetic energy for cavitation number *(σ/σ_i=1.06)(a) at x/d=0.6 (b) at x/d=3.*

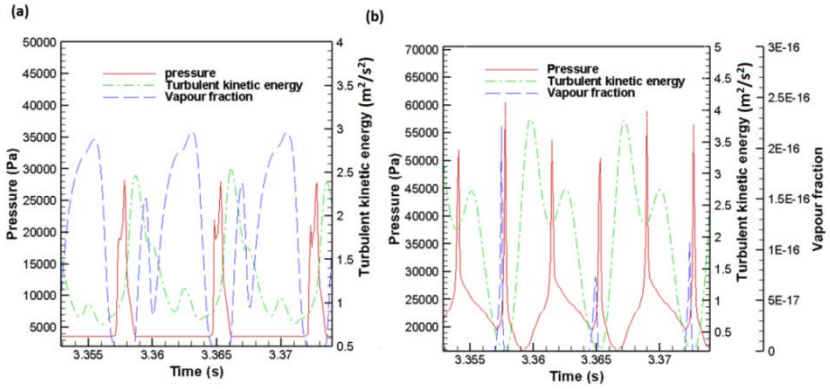

Figure 6: Variation of pressure, turbulent kinetic energy and vapour fraction for cavitation number (σ/σ_i=0.5))(a) at x/d=0.6 (b) at x/d=3.

leads to a significant reduction in turbulent kinetic energy. However, in case of cavitation (figure 6(b)), turbulent kinetic energy peak value actually increases when compared with that at the near cylinder (figure 6(a)). Also similar to near cylinder case presented in figure 6 (a), there is an increase in turbulent kinetic energy and pressure along with a reduction in vapour content. Thus figure 4 and figure 6 together present a picture of an energy exchange —

turbulent kinetic energy is used for the growth of a cavity while a collapsing cavity leads to an increase in turbulent kinetic energy.

4. Conclusion

Numerical results agreed with the experiment in terms of mean pressure, base pressure fluctuations and corresponding frequency. The reduction of shedding frequency with cavitation number is explained in terms of vorticity. The variation of mean pressure, vapour fraction and turbulent kinetic energy contour and plots for different cavitation number suggest the presence of an energy interaction in which local turbulence promotes bubble formation and growth and there is an increase in turbulent intensity in regions of cavity collapse due to recovery of mean pressure.

References

[1] Roshko, A. (1961). *Experiments on the flow past a circular cylinder at very high Reynolds number*. J. Fluid Mech., 10, 345–356.

[2] Schewe, G. (1983). *On the force fluctuations acting on a circular cylinder in cross-flow from subcritical up to transcritical Reynolds numbers*. J Fluid Mech., 133, 265–285.

[3] Sumer, B. M. and Fredsoe J.(2006). *Hydrodynamics around cylindrical structures*. World Scientific Publishing Ltd., Singapore.

[4] Achenbach, E. (1968). *Distribution of local pressure and skin friction around a circular cylinder in cross-flow upto Re = 5 x* 10^5. J. Fluid Mech., 34(4), 625–639.

[5] Bearman, P. W. (1969). *On vortex shedding from a circular cylinder in the critical Reynolds number regime*. J. Fluids. Mech., 37, 577–585.

[6] Norberg, C. (1994). *An experimental investigation of the flow around a circular cylinder*: *influence of aspect ratio*. J. Fluid Mech., 258, 287–316.

[7] Wykes, M. E. P. (1978). *Experimental studies of viscous effects on cavitation.* Ph.D. thesis, St. John's College, University of Oxford, United Kingdom.

[8] Ramamurthy, A. and Bhaskaran P. (1977). *Constrained flow past cavitating bluff bodies*. ASME J. Fluids Eng., 99, 717–726.

[9] Ihara, A. and Murai H.(1986). *Cavitation inception on a circular cylinder at critical and* supercritical flow range. ASME, J. Fluids Eng., 108, 421–427.

[10] Matsudaira, Y., Gomi Y., and Oba R.(1992). *Characteristics of bubble-collapse pressures in a karman-vortex cavity*. JSME INT. J., Ser. II, 35, 179–185.

[11] Saito, Y. A. and Sato K.,(2003). Cavitation bubble collapse and impact in the wake of circular cylinder. 5th Int. Symposium on Cavitation (CAV2003), Osaka, Japan.

[12] Kunz, R. F., Boger D.A., Stinebring D.R., Chyczewski T.S., Lindau J.W., Gibeling H.J., Venkateswaran S. and Govindan T. (2000). *A preconditioned navier stokes method for two-phase flows with application to cavitation prediction*. Comput. Fluids, 29, 849875.

[13] Schnerr, G. H. and Sauer J. (2001). *Physical and numerical modeling of unsteady cavitation dynamics*. 4th int. conference on multiphase flow, Orleans, USA.

[14] Singhal, A. K., Athavale M., Li H., and Jiang Y.(2002). *Mathematical basis and validation of the full cavitation model*. J. Fluids Eng., 124, 617–624.

[15] Seo, J. H., Moon Y.J., and Shin B. R. (2008). *Prediction of cavitating flow noise by direct numerical simulation*. J. Comput. Phys., 13, 65116531.

[16] Gnanaskandan, A. and Mahesh K.(2016). *Numerical investigation of near-wake characteristics of cavitating flow over a circular cylinder*. J. Fluid Mech, 790, 453–491.

[17] Unal, M. F. and Rockwell D. (1988). *On the vortex formation from a cylinder part 1.the initial instability*. J. Fluid Mech., 190, 91–512.

[18] Menter, F. (1994). *Two equation eddy viscosity turbulence models for engineering applications*. AIAA J., 32, 1598–1605.

[19] Kumar P., Bakshi S. and Chatterjee D.(2017). *Experimental investigation of cavitation behind the circular cylinder* J. Thermal Sci. Eng. App., ASME, 9(3), 031004-1-6.

[20] Young, J. O. and Hall W. J.(1966). *Effects of cavitation on periodic wakes behind symmetric wedges*. ASME, J. Basic Eng., 88, 163–176.